Published in final edited form as:
Nucl Med Biol. 2008 August ; 35(6): 655–663. doi:10.1016/j.nucmedbio.2008.05.001.

Evaluation of a Bromine-76 Labeled Progestin 16α,17α-dioxolane for Breast Tumor Imaging and Radiotherapy: *in vivo* Biodistribution and Metabolic Stability Studies

Dong Zhou[1], **Terry L. Sharp**[1], **Nicole M. Fettig**[1], **Hsiaoju Lee**[1], **Jason S. Lewis**[1], **John A. Katzenellenbogen**[2], and **Michael J. Welch**[1]

1*Mallinckrodt Institute of Radiology, Washington University School of Medicine, St. Louis, MO 63110, USA.*

2*Department of Chemistry, University of Illinois, Urbana, IL 61801, USA.*

Abstract

Introduction—Progesterone receptors (PRs) are present in many breast tumors, and their levels are increased by certain endocrine therapies. They can be used as targets for diagnostic imaging and radiotherapy.

Method—16α,17α-[(R)-1'-α-(5-[^{76}Br]bromofurylmethylidene)dioxyl]-21-hydroxy-19-norpregn-4-ene-3,20-dione ([^{76}Br]**3**), a PR ligand with relative binding affinity (RBA) = 65 and log P*o/w* = 5.09 ± 0.84, was synthesized via a two-step reaction and its tissue biodistri0bution and metabolic stability were evaluated in estrogen-primed immature female Sprague-Dawley rats.

Results—[^{76}Br]**3** was synthesized in 5% overall yield with specific activity being 200~1250 Ci/mmol. [^{76}Br]**3** demonstrated high PR-mediated uptake in the target tissue uterus (8.72 ± 1.84 %ID/g at 1 h) that was reduced by a blocking dose of unlabeled progestin R5020, but the non-specific uptake in blood and muscle (2.11 ± 0.14 and 0.89 ± 0.16 %ID/g at 1 h, respectively) was relatively high. [^{76}Br]**3** was stable in whole rat blood *in vitro*, but it was not stable *in vivo* due to the fast metabolism that occurred in the liver, resulting in the formation of a more polar radioactive metabolite and free [^{76}Br]bromide. The level of free [^{76}Br]bromide in blood remained high during the experiment (2.11 ± 0.14 %ID/g at 1 h and 1.52 ± 0.24 %ID/g at 24 h). The tissue distribution of [^{76}Br]**3** at 1 and 3 hours was compared with that of the ^{18}F analogs, [^{18}F]FFNP **1** and ketal **2**.

Conclusion—[^{76}Br]**3** may have potential for imaging PR positive breast tumors at early time points, but it is not suitable for imaging at later times or for radiotherapy.

Keywords

progesterone receptor; Br-76 radiolabeling; PET breast tumor imaging; radiotherapy

1. Introduction

Steroid receptors are found in a number of endocrine-responsive cancers, estrogen receptors (ERs) and progesterone receptors (PRs) in many breast tumors and androgen receptors (ARs)

Corresponding author: Michael J. Welch, PhD, Mallinckrodt Institute of Radiology, Washington University School of Medicine, St. Louis, MO 63110, USA, Tel: +1 314 362 8436 Fax: +1 314 362 8399, E-mail address: welchm@wustl.edu.

in most prostate cancers. These receptors serve as targets for endocrine therapies of these cancers, but they also can be used as targets for diagnostic imaging and radiotherapy. Diagnostic imaging can be achieved by the administration of a suitably radiolabeled ligand that accumulates in the receptor-positive tumor, where it can be detected and quantified by imaging. Such images can sometimes be used to predict whether hormone therapy will be effective [1–4]. In a related manner, a hormone receptor ligand labeled with a radionuclide (e.g., an Auger electron emitting isotope) that accumulates in a tumor through a receptor-mediated uptake process can deliver a cytotoxic dose of high linear energy transfer (LET) radiation selectively to the tumor cells, ablating the tumor while limiting widespread radiation toxicity. Therefore, the development of such hormone receptor ligands for both diagnostic imaging and radiotherapy is a promising area of research.

Diagnostic imaging of breast and prostate tumors by positron emission tomography (PET) is well established and has been achieved using steroids labeled with fluorine-18, such as 16α-[^{18}F]fluoroestradiol (FES) [3,4] for breast tumor imaging and 16β-[^{18}F]fluoro-5α-dihydrotestosterone (FDHT) [5,6] for prostate cancer imaging. Although a number of steroids labeled with bromine and iodine radioisotopes have been prepared [7–12] and studied, especially in terms of their potential for selective radiotherapy, their use in imaging studies, particularly in humans, has been more limited [12]. Nevertheless, previous studies have established the feasibility of using various Auger electron-emitting isotopes for selective cellular therapy [13–23].

Bromine-76 decays with a significant amount of positron emission (57% positron and 43% electron capture), a characteristic that allows for diagnostic PET imaging to be used to complement the use of this isotope in radiotherapy. It can conveniently be produced via the ^{76}Se(p,n)^{76}Br reaction on the majority of medical cyclotrons [24]. ^{76}Br has a half life of 16.2 hours, which is long enough to permit target tissue-selective distribution while being sufficiently short so that the bulk of the dose can be delivered to the tissue prior to metabolism and elimination of the radiopharmaceutical. Because the natural abundance of bromine is low, organic compounds can be labeled with very high specific activity (SA), which is a general requirement for the study of receptor-binding related biological processes.

In principle, a ligand based on binding to either ER or PR might be used in applications of breast tumor imaging and therapy in an untreated patient. However, a PR-based radioligand has some potential advantages over an ER-based one: (1) there is a better correlation between PR status and hormonal responsiveness than there is with ER status [25–29]; (2) a PR-based ligand could be used after the initiation of anti-estrogen hormonal therapy, whereas an ER-based one would not be useful when tumor ER is saturated by the hormonal agent [30]. Moreover, (3) PR-based ligands may benefit from the increased PR levels induced by the transient agonistic effect of tamoxifen during the initial course of tamoxifen treatment of breast tumor [31–33].

A series of bromine-and iodine-substituted 16α,17α-dioxolane progestins have been synthesized [34] based on the very promising PR ligand, fluoro furanyl norprogesterone (FFNP) **1** [35] and its analog **2** [36]. Among this series, 16α,17α-[(R)-1'-α-(5-bromofurylmethylidene)dioxyl]-21-hydroxy-19-norpregn-4-ene-3,20-dione (**3**) appeared to be the most promising one with good relative binding affinity to PR (RBA = 65, relative to R5020) and moderate lipophilicity (log $P_{o/w}$ = 5.09 ± 0.84) [34]. In this report, we describe the ^{76}Br radiolabeling of **3**, the *in vivo* biodistribution and metabolic stability studies of **3** in estrogen-primed immature female Sprague-Dawley rats as a potential agent for breath tumor imaging and radiotherapy.

2. Materials and methods

2.1 General

^{76}Br was produced at the Washington University cyclotron facility by the ^{76}Se(p,n)^{76}Br nuclear reaction on a ^{76}Se-enriched Cu_2Se target. ^{76}Br was recovered via a modified dry distillation method [24]. The radionuclide was in the form of [^{76}Br]NH_4Br in 0.6 M NH_4OH. The solution was filtered through a C-18 Sep-Pak light cartridge (Waters Corp.) and blown down to dryness under very mild N_2 flow at 130°C. High performance liquid chromatography (HPLC, Dionex, Sunnyvale, CA, USA) was performed with an ultraviolet detector operating at 231 nm and a radioactive detector. Agilent Zorbax SB-C18 250 × 4.6 mm 5 μm analytical column and Agilent Zorbax SC-C18 250 × 9.4 mm 5 μm semi-preparative column were used for analysis and preparative purification respectively. Acetonitrile and water were used as the HPLC mobile phase. RadioTLC was performed using a Bioscan System 2000 imaging scanner (Bioscan, Washington, DC, USA). All chemicals and solvents were obtained from common commercial sources. Compound **4** [37] and **6** [34,38] were synthesized according to previously published literature. All animal experiments were conducted in compliance with the Guidelines for the Care and Use of Research Animals published by the Animal Studies Committee of Washington University in St. Louis, School of Medicine.

2.2 Radiochemistry

~10 mCi [^{76}Br]NH_4Br was dried in a 5 mL Wheaton V vial at 130°C under very gentle N_2 flow. At ambient temperature, 20 μL acetic acid and 0.5 mg **4** in 50 μL methanol were added, and the solution was vortexed before addition of 100 μL 2 : 1 hydrogen peroxide/acetic acid (pre-mixed for at least 4 hours). Then the reaction mixture was vortexed to homogeneity. Upon the completion of the reaction in 30 minutes (> 80% incorporation according to radio-TLC analysis: silica plate (EMD Cat. 15341–5), 1 : 1 ethyl acetate/hexanes, R_f = 0.8), the reaction was quenched by the addition of 2 mL water. The reaction mixture was extracted with 0.7 mL × 2 dichloromethane, which was loaded onto a column (I.D. 0.5 cm, from bottom to top: 2 cm $MgSO_4$, 4 cm silica, 2 cm Na_2SO_4, and 1 cm sand, filled with dichloromethane). [^{76}Br]**5** was eluted with dichloromethane, and the eluent was collected in 1 mL portions. The two portions containing the majority of ^{76}Br radioactivity (3.5 mCi, 35% isolated yield) were transferred to a 10 mL Pyrex screw-capped tube containing 1.2 mg **6**, and the solution was concentrated to 1.0 mL under a flow of N_2 at ambient temperature. Then 18.0 μL 1 : 1 triethyl orthoformate (TEOF)/CH_2Cl_2 was added followed by the addition of 2.0 μL 70% $HClO_4$. After the solution was vortexed, the color of the reaction changed to pale pink, deepening slightly in color at 30 minutes, at which point more than 80% of [^{76}Br]**5** was converted to[^{76}Br]**3** (2 : 1 ethyl acetate/hexanes, R_f = 0.4). The reaction mixture was first quenched by the addition of small amount of $NaHCO_3$ (right after the tube was opened to the air) and then it was passed through a light alumina Sep-Pak (Waters Corp.), followed by rinsing with 2 mL dry dichloromethane. 2 mCi of radioactivity was collected in dichloromethane, which was subsequently removed under a flow of N_2 at ambient temperature. The dried radioactivity was reconstituted in 100 μL dimethyl formide, 700 μL acetonitrile and 1200 μL water and injected for HPLC purification. The reverse phase HPLC purification (Agilent Zorbax SC-C18 250 × 9.4 mm 5 μm) was carried out using 47.5% acetonitrile 52.5% water at a flow rate of 3 mL/min and UV at 231 nm. Radioactivity was monitored by a radioactivity detector (Bioscan, B-FC-3200), and 600 μCi [^{76}Br]**3** was collected at 25.6 minutes. The HPLC collection of [^{76}Br]**3** was diluted in 30 mL water, and the solution was passed through a C18 classic Sep-Pak (preconditioned with 6 mL methanol and 12 mL water) to trap the activity. After the Sep-Pak was rinsed with 10 mL water, [^{76}Br]**3** was eluted with 1 mL ethanol. The ethanol solution of [^{76}Br]**3** was concentrated in order to make a final solution of 1.2 mL of 15% ethanol and 85% saline. Specific activity was determined to be more than 400 Ci/mmol (EOS) using reverse phase HPLC (Agilent Zorbax

SB-C18 250 × 4.6 mm 5 μm) applying 60% acetonitrile and 40% water as solvents at a flow rate of 1.5 mL/min and UV at 231 nm.

2.3 In vitro stability study

An *in vitro* stability study was carried out in isolated heparinized whole rat blood (Sprague-Dawley rats, mature). The whole blood (5 mL) was incubated with ~3 μCi [^{76}Br]**3** in 20 μL ethanol for 5 min, 30 min, 1 h and 2 h at 37°C. An aliquot of blood was treated with 3 volumes of ethanol at each time point, and the lysed sample was centrifuged to separate the supernatant from the pellet. The radioactivity in the supernatant and the pellet was counted separately on a Beckman Gamma 8000 well counter. The radioactive species in the supernatant was analyzed by Silica TLC using 2 : 1 ethyl actate/hexanes as the developing solvent (R_f = 0.4 for [^{76}Br]**3**) and co-elution with non-radioactive **3**.

2.4 In vivo metabolic stability study

The metabolism of [^{76}Br]**3** was evaluated in estrogen-primed immature female Sprague-Dawley rats (24 h and 3 h estradiol treatment before injection, n = 1) by injection of 30 μCi of [^{76}Br]**3** in 15% ethanol/saline via the tail vein. The rats were sacrified at 1 min, 1 h, 3 h, and 24 h post-injection and blood, muscle, liver, and uterus were collected. Tissue samples were homogenized in 1 mL buffer at room temperature. The supernatant and pellet were separated by centrifugation and kept in ice to prevent degradation of the samples. The radioactive species in the supernatant was analyzed by silica gel TLC using Bioscan system 2000 imaging scanner. The samples were co-spotted with non-radioactive **3** and TLC was developed in ethyl acetate (R_f = 0, 0.6 for [^{76}Br]bromide and [^{76}Br]**3** respectively). The radioactivity in the supernatant and the pellet was counted separately as mentioned above.

2.5 In vivo tissue biodistribution studies

PR levels in the uteri of immature female Sprague-Dawley rats (25 days old, ~50 g) were induced by daily subcutaneous injections for 1 or 2 days of 5 μg of estradiol in 0.1 mL of 20% ethanol/80% sunflower seed oil. The experiments were begun 24 h (or 3 h) after the last injection. The HPLC purified [^{76}Br]**3** was injected in 100~150 μL 15% ethanol/saline via the tail vein of 2% Isoflurane anesthetized rats. At the specified time points post-injection, the rats were sacrificed by cervical dislocation, and blood, tissues and organs were removed, weighed, and counted in a Beckman Gamma 8000 counter. To determine whether the uptake was mediated by a high-affinity, limited-capacity system, one set of animals was co-injected with [^{76}Br]**3** together with 18 μg of R5020 in order to fully occupy the progesterone receptors.

3. Results

3.1 Radiochemistry

[^{76}Br]**3** was synthesized by two steps: aromatic electrophilic substitution of the tributyltin precursor **4** to afford [^{76}Br]**5** using 2 : 1 hydrogen peroxide/acetic acid as oxidizing agent and acetalization of progestin 16α,17α,21-triol **6** with [^{76}Br]**5** in the presence of 70% $HClO_4$ and TEOF to afford an endo isomer **3** and an exo isomer **7** in 1 : 1 ratio (Fig. 2). The yields for both the incorporation of [^{76}Br]bromide and the acetalization of **6** were up to 80%, but the overall yield of [^{76}Br]**3** was only 5% (not decay corrected). [^{76}Br]**3** was purified by reversed phase C18 HPLC and confirmed by co-elution with non-radioactive **3**. The specific activity was determined by HPLC to be from 200 to 1250 mCi/μmol at the end of synthesis.

3.2 In vitro stability study

[^{76}Br]**3** was stable in HPLC solvent overnight, showing no sign of radiolysis due to the high energy radiation of the ^{76}Br isotope. The *in vitro* stability study was carried out in isolated

whole rat blood. Around 75% of the radioactivity was separated into the supernatant from the pellet over the period of 2 hours, indicating little binding of [^{76}Br]**3** to cells or cellular proteins in the blood. According to the radioTLC analysis of the supernatant, [^{76}Br]**3**, confirmed by co-elution with co-spotted non-radioactive **3** on TLC, was the only radioactive species observed during the experiment (2 hours), indicating good *in vitro* stability of [^{76}Br]**3** in rat blood.

3.3 In vivo metabolic stability study

An *in vivo* metabolic stability study was carried out in estrogen-primed immature female Sprague-Dawley rats, the same animal model used in the tissue biodistribution (Table 1). Around 90%, 90%, 80%, and 75% of radioactivity was found in the supernatants from uterus, muscle, blood, and liver extraction samples during the experiment (24 h), indicating little binding of [^{76}Br]**3** to cells or cellular proteins in the animal. There was slightly less recovery of radioactivity from blood and liver. At 1 minute after administration of [^{76}Br]**3**, metabolism was observed in the liver: 58.5% radioactivity in the supernatant remained as [^{76}Br]**3** (R_f = 0.6), 27% as [^{76}Br]bromide (R_f = 0) and 14.5% as a more polar metabolite (**8**, R_f = 0.3, structure unknown); no metabolism was observed in the blood, muscle and uterus supernatants at 1 minute. At 1 h post-injection, 31.5% of the radioactivity in the liver supernatant was observed to be [^{76}Br]**3**; the other radioactivity was the more polar metabolite **8** and [^{76}Br]bromide; 66.5% of the radioactivity in the blood supernatant was [^{76}Br]bromide, with only 9% as [^{76}Br]**3** and 24.5% as the more polar metabolite **8**; 60% and 80% radioactivity in the muscle and uterus supernatants remained as [^{76}Br]**3**, respectively, with the rest being [^{76}Br]bromide. At 3 h post-injection, 19.5% of activity was still [^{76}Br]**3** in the liver supernatant, but the majority of radioactivity in the blood supernatant was free [^{76}Br]bromide; the amount of [^{76}Br]**3** in the muscle and uterus supernatants remained high (68% and 67.5%, respectively). At 24 hours post-injection, the amount of radioactivity in liver and muscle was under the detection limit for radio-TLC analysis; free[^{76}Br]bromide was the only radioactivity observed in the blood supernatant; there was still 40% as [^{76}Br]**3** in the uterus supernatant with the rest as [^{76}Br] bromide.

3.4 Tissue biodistribution studies

0.5~40 μCi HPLC-purified [^{76}Br]**3** at a specific activity of 200~1250 mCi/μmol was injected into estrogen-primed immature female Sprague-Dawley rats. Table 2 shows the %ID/g uptake of radioactivity data using 7 μCi [^{76}Br]**3** at a specific activity of more than 400 mCi/μmol. Initially, at 15 min post-injection, the highest uptake was observed in the uterus (8.22 ± 0.6 % ID/g), which is the most PR-rich target organ; the uptake in liver and muscle was 4.22 ± 0.87 and 1.38 ± 0.23 %ID/g, respectively. At 1h post-injection, uptake in the uterus remained high (8.72 ± 1.84 %ID/g), while up to 50% of the radioactivity in liver and muscle was washed out; the activity in blood was similar to that at 15 min. At 3 h post-injection, uptake in the uterus was reduced to 5.52 ± 1.84 %ID/g, and the uptake in liver and muscle was reduced further. However, the activity in blood remained constant. At 24 h post-injection, all tissue activities were reduced to background, with the highest activity in blood.

To determine whether the uptake was mediated by a high-affinity, limited-capacity system, a blocking study was carried out by co-injection of 2~3 μCi [^{76}Br]**3** at a specific activity of 1250 mCi/μmol together with 18 μg R5020 (RBA = 100) to fully occupy the progesterone receptors; the results are shown in Table 3. The uptake in uterus and ovaries of the blocked animals was reduced 54% and 42%, respectively, lowering to the level seen in non-target tissues, indicating that the uptake of [^{76}Br]**3** in the uterus is mediated by binding to PR. No obvious differences in activity levels were observed in blood, liver, spleen and muscle between the blocked and non-blocked animals, and the uptake values reported in Table 3 are similar to those in Table 2 at 1 and 3 h post-injection.

To establish that the uptake was not limited by undetected PR-binding non-radioactive impurities, 0.8, 2 and 40 μCi [^{76}Br]**3** at a specific activity of 200 mCi/μmol was injected into a set of animals, and the tissue biodistribution was determined at 1 h post-injeciton. The results are shown in Table 4. The uptake in the organs or tissues tested showed no statistical difference from the 'low' to the 'high' dose administration at 1 h post-injection. Also, these biodistribution data are similar to those reported in Table 2 and 3. These results indicate that the effective specific activity of the HPLC-purified [^{76}Br]**3** is not low and that PR-binding impurities are not a limiting factor in the biodistribution of [^{76}Br]**3**.

4. Discussion

Unlike the extensive imaging studies that have been performed using ER radio-ligands [39], the study of PR ligands as imaging agents or for radiotherapy has been limited. Nevertheless, the most promising PR ligand for PET imaging of breast cancer reported so far is fluoro furanyl norprogesterone (FFNP, **1**), the ^{18}F-labeled form of which is undergoing clinical imaging investigations at Washington University, School of Medicine. FFNP has a high relative binding affinity to PR, low nonspecific binding, and a high binding selectivity index [35,40]. In tissue biodistribution studies, [^{18}F]FFNP demonstrated high PR-selective uptake in the principal PR target organs, uterus and ovaries, and relatively low uptake in non-PR target tissues, such as fat and bone [35]. In addition, FFNP is expected to be more stable towards the metabolism of the C-20 ketone by steroid dehydrogenases, because it is protected by the bulk of the 16α, 17α-furanyl group, a group onto which a bromine can be introduced easily. The favorable pharmacokinetic and pharmacodynamic features of FFNP meet the requirements for a successful ligand for imaging or therapy [40]. Therefore, 16α,17α-[(R)-1'-α-(5-bromofurylmethylidene)dioxyl]-21-13 hydroxy-19-norpregn-4-ene-3,20-dione (**3**) was developed, because when labeled with bromine-76, it has potential as a PR ligand for imaging and radiotherapy based on the favorable characteristics of FFNP (**1**) and its predecessor ketal **2**.

The synthesis of the tributyltin precursor for direct labeling of [^{76}Br]**3** via electrophilic radiobromination failed to afford the desired product. Therefore, the two-step synthesis of [^{76}Br]**3** was adopted from the previously reported method [36]. The radiobromination of **5** proceeded very well to afford more than 80% incorporation using 1 : 1 hydrogen peroxide/ acetic acid (premixed 4 hours); however, the isolated yield was low because of the instability of the furfural group towards acid and low recovery from the silica gel column. The acetalization was a challenging step [36]. The reaction was optimized to afford up to 80% conversion of [^{76}Br]**5** using 9 μL TEOF, 2 μL 70% $HClO_4$ in 1 mL dichloromethane. The major problem with this acetalization reaction was the rapid formation of a more polar radioactive unknown, the formation of which was also observed in the previously reported method [36]. It was found necessary to separate the desired product from the reagents before it became converted to the unknown byproduct completely. After Alumina Sep-Pak filtration, the desired products were very stable as in a dichloromethane solution. The low overall yield of [^{76}Br]**3** was partially due to the formation of the two isomers, endo **3** and exo **7**, in addition to workup conditions that were not fully optimized. The specific activity was determined by HPLC, and while impurities coeluting with [^{76}Br]**3** might have lowered the effective specific activity of this compound, tissue distribution studies indicated that the effective specific activity of [^{76}Br]**3** was not a limiting factor.

Metabolic stability is an issue facing the development of PR-based steroid ligands [41–43]. The C-20 ketone in progestins is at risk for reduction to a C-20 hydoxy group, giving a compound with very low affinity for PR that is inactive *in vivo* and would thus be unsuitable as a progestin radiotracer imaging agent. The *in vitro* stability test of [^{76}Br]**3** in whole rat blood showed that it was stable, presumably because the C-20 ketone was protected by the 16α,

17α-dioxolane group in **3**. However, *in vivo* metabolic stability studies of [^{76}Br]**3** in estrogen-primed immature female Sprague-Dawley rats demonstrated that it underwent rapid metabolism in the liver, giving two metabolites, free [^{76}Br]bromide and a more polar unidentified metabolite **8** that were evident as early as 1 minute. The structure of the more polar unknown **8** was not determined, but is likely to be the C-20 hydroxy analog of **3**, based on its greater hydrophilicity and reports of this conversion in compounds with similar structure [42]. Free [^{76}Br]bromide appeared to be the final metabolite *in vivo*.

Despite the rapid metabolism of [^{76}Br]**3** in the liver, as early as 1 minute post injection, there appeared to be no appearance of metabolites of [^{76}Br]**3** in the blood *in vivo* (also, as noted above, no metabolism was observed in whole rat blood at 2 hours *in vitro*). Nevertheless, by 1-hour post-injection, when [^{76}Br]**3** had undergone extensive metabolism in liver, there were only low levels of unconverted [^{76}Br]**3** in the blood and high level of metabolites. At later times, metabolites also began to appear in muscle and uterus, although there was substantial retention of unconverted [^{76}Br]**3** remained in the uterus, where it is presumably protected from metabolism by its binding to PR. The target tissue protection of receptor binding radiopharmaceuticals has been noted before with ER ligands [43–45]. The rapid metabolism we have observed is not surprising, because liver is known to be the major site of steroid metabolism [46] and the C-21 hydroxy group in [^{76}Br]**3** might facilitate the reduction of the C-20 ketone.

Tissue distribution studies of [^{76}Br]**3** demonstrated high uptake in the target tissues, uterus and ovaries, that was shown to be PR specific by selective displacement by a blocking dose of the potent progestin R5020. Uptake in non-PR target tissues, however, was not low, particularly at early times. This high, initial non-specific uptake is likely due to the relatively high lipophilicity of **3** [40] compared with that of FFNP **1** (Table 5). At later times, the metabolites of [^{76}Br]**3**, especially free [^{76}Br]bromide, are likely contributors to the non-target tissue activity because within 1 hour post-injection, these species constitute the majority of the circulating activity. It is of note that [^{76}Br]bromide is known to distribute rapidly [47] and non-specifically [48] and to be retained in blood for long periods of time [47].

Despite the high initial uptake of [^{76}Br]**3** by non-target tissues, the radioactivity in uterus was retained very well from 1 minute to 1 hour, thereafter washing out more slowly than was observed in non-target tissues. This selective retention of uterine activity following [^{76}Br]**3** injection is further evidence that a large proportion of its interaction in the uterus is due to the presence of PR. Furthermore, at 1 hour post-injection, the ratio of activity in the uterus compared to muscle following [^{76}Br]**3** injection was comparable to that of FFNP (Table 5), and a good ratio was maintained out to 3 hours, declining, not surprisingly by 18–24 hours. Uterus to blood ratios were lower, however, presumably because of the increasing fraction of free [^{76}Br]bromide that was being retained in the blood. The selective uptake and retention of [^{76}Br]**3** in target tissues is impressive, considering that its PR binding affinity is relatively low, being 65 (compared to 100 for R5020 and 190 for FFNP; Table 5) and the declining levels of circulating [^{76}Br]**3** that results from its rapid metabolism in liver. The bromofuranyl group in [^{76}Br]**3** appears to be a metabolic liability that is responsible for the rapid production of free [^{76}Br]bromide. Thus, metabolism may render imaging agents that contain this functionality ineffective and cause therapeutic agents to become harmful to non-target tissues from a dosimetry point of view.

It is instructive to compare [^{76}Br]**3** with FFNP **1** and the C-21 hydroxy ketal analog **2** (the predecessor of FFNP) in terms of their *in vivo* biodistribution (Table 5 and Figure 1). Among them, **3** has the lowest relative binding affinity but the highest lipophilicity (log $P_{o/w}$). Interestingly, the uterus uptake of [^{76}Br]**3** was comparable to that of **1** and even better than that of **2** at 1 hour post-injection, but the blood and muscle uptake at 1 hour post-injection was

much higher than those of **1** and **2** because of the lipophilicity of [^{76}Br]**3**. The known routes of metabolism and excretion of steroids are liver and kidney. The liver uptake was the lowest for **3**, but the kidney uptake was very high. The similarities between the uptake of [^{76}Br]**3** and FFNP **1** at 1 hour post-injection diminish with time (compare 1 h and 3 h), because of the extensive metabolism of [^{76}Br]**3**. Thus, while the uterine activity of compounds **1** and **2** remain the same, and their uterus to blood and muscle ratios increase with time, these values decrease with [^{76}Br]**3**. Thus, it is likely that compound **1** has greater metabolic stability than [^{76}Br]**3**, perhaps the result of the C-21 fluorine further stabilizing the C-20 ketone [49].

In summary, [^{76}Br]**3** has high PR-mediated uptake in the target tissues, however, the high uptake in blood and muscle may cause problems for imaging and radiotherapy. The metabolic stability of **1** and **2** was not studied, so no direct comparison can be made between them and [^{76}Br]**3**. However, the stability of [^{76}Br]**3** is comparable to that of 16α-[^{18}F]fluoroestradiol (FES) [50], suggesting that [^{76}Br]**3** has some potential for PET imaging of PR in breast tumors.

5. Conclusion

16α,17α-[(R)-1'-α-(5-[^{76}Br]bromofurylmethylidene)dioxyl]-21-hydroxy-19-norpregn-4-ene-3,20-dione ([^{76}Br]**3**) was successfully synthesized, and its tissue biodistribution and metabolic stability were evaluated in estrogen-primed immature female Sprague-Dawley rats. [^{76}Br]**3** demonstrated high PR-mediated uptake in the target tissues that was blocked by excess unlabeled progestin, but the activity in blood and muscle was also relatively high because of the high lipophilicity of [^{76}Br]**3** and the subsequent formation of metabolites. [^{76}Br]**3** was metabolized quickly in the liver, but not in blood, to form a more polar radioactive metabolite and free [^{76}Br]bromide. Despite the favorable initial biodistribution of [^{76}Br]**3**, these subsequent metabolism events render this compound unsuitable as an imaging agent at later time points and for radiotherapy applications that would require specific and prolonged target tissue retention.

Acknowledgment

This work was supported by the DOE (DE FG02 86ER60401 to JAK and DE FG02-84ER-60218 to MJW) and the NIH (PHS 2R01 CA25836 to JAK).

References

1. Dehdashti F, Flanagan FL, Mortimer JE, Katzenellenbogen JA, Welch MJ, Siegel BA. Positron emission tomographic assessment of "metabolic flare" to predict response of metastatic breast cancer to antiestrogen therapy. Eur J Nucl Med 1999;26:51–56. [PubMed: 9933662]
2. Mortimer JE, Dehdashti F, Siegel BA, Trinkaus K, Katzenellenbogen JA, Welch MJ. Metabolic flare: indicator of hormone responsiveness in advanced breast cancer. J Clin Oncol 2001;19:2797–2803. [PubMed: 11387350]
3. Mortimer JE, Dehdashti F, Siegel BA, Katzenellenbogen JA, Fracasso P, Welch MJ. Positron emission tomography with 2-[^{18}F]fluoro-2-deoxy-D-glucose and 16α-[^{18}F]fluoro-17β-estradiol in breast cancer: Correlation with estrogen receptor status and response to systemic therapy. Clin Cancer Res 1996;2:933–939. [PubMed: 9816253]
4. Jonson SD, Bonasera TA, Dehdashti F, Cristel ME, Katzenellenbogen JA, Welch MJ. Comparative breast tumor imaging and comparative in vitro metabolism of 16α-[^{18}F]fluoroestradiol-17β and 16β-[^{18}F]fluoromoxestrol in isolated hepatocytes. Nucl Med Biol 1999;26:123–130. [PubMed: 10096512]
5. Larson SM, Morris M, Gunther I, Beattie B, Humm JL, Akhurst TA, et al. Tumor localization of 16β-^{18}F-fluoro-5α-dihydrotestosterone versus ^{18}F-FDG in patients with progressive, metastatic prostate cancer. J Nucl Med 2004;45:366–373. [PubMed: 15001675]

6. Dehdashti F, Picus J, Michalski JM, Dence CS, Siegel BA, Katzenellenbogen JA, et al. Positron tomographic assessment of androgen receptors in prostatic carcinoma. Eur J Nucl Med Mol Imaging 2005;32:344–350. [PubMed: 15726353]
7. McElvany KD, Welch MJ, Katzenellenbogen JA. Radiobrominated estrogen receptor-binding radiopharmaceuticals for breast tumor imaging. Nucl Med Biol Adv, Proc World Congr 3rd 1983;4:3610–3613.
8. Senderoff SG, McElvany KD, Carlson KE, Heiman DF, Katzenellenbogen JA, Welch MJ. Methodology for the synthesis and specific activity determination of 16α-[^{77}Br]-bromoestradiol-17β and 16α-[^{77}Br]-bromo-11β-methoxyestradiol-17β, two estrogen receptor-binding radiopharmaceuticals. Int J Appl Radiat Isot 1982;33:545–551. [PubMed: 6889575]
9. Katzenellenbogen JA, McElvany KD, Senderoff SG, Carlson KE, Landvatter SW, Welch MJ. 16α-[^{77}Br]bromo-11β-methoxyestradiol-17β: a gamma-emitting estrogen imaging agent with high uptake and retention by target organs. J Nucl Med 1982;23:411–419. [PubMed: 7077395]
10. Katzenellenbogen JA, Senderoff SG, McElvany KD, O'Brien HA Jr, Welch MJ. 16α-[bromine-77] bromoestradiol-17β: a high specific-activity, gamma-emitting tracer with uptake in rat uterus and induced mammary tumors. J Nucl Med 1981;22:42–47. [PubMed: 6778976]
11. Landvatter SW, Katzenellenbogen JA, McElvany KD, Welch MJ. (2R*,3S*)-1-[^{125}I]Iodo-2,3-bis(4-hydroxyphenyl)pentane ([^{125}I]iodonorhexestrol) and (2R*,3S*)-1-[^{77}Br]Bromo-2,3-bis(4-hydroxyphenyl)pentane ([^{77}Br]bromonorhexestrol), two gamma-emitting estrogens that show receptor-mediated uptake by target tissues in vivo. J Med Chem 1982;25:1307–1312. [PubMed: 6292424]
12. McElvany KD, Katzenellenbogen JA, Shafer KE, Siegel BA, Senderoff SG, Welch MJ. 16 alpha-[^{77}Br]bromoestradiol: dosimetry and preliminary clinical studies. J Nucl Med 1982;23:425–430. [PubMed: 7077397]
13. Bronzert DA, Hochberg RB, Lippman ME. Specific cytotoxicity of 16 alpha-[^{125}I]iodoestradiol for estrogen receptor-containing breast cancer cells. Endocrinology 1982;110:2177–2182. [PubMed: 7075553]
14. Bloomer WD, McLaughlin WH, Milius RA, Weichselbaum RR, Adelstein SJ. Estrogen receptor-mediated cytotoxicity using iodine-125. J Cell Biochem 1983;21:39–45. [PubMed: 6874726]
15. McLaughlin WH, Pillai KM, Edasery JP, Blumenthal RD, Bloomer WD. [^{125}I]iodotamoxifen cytotoxicity in cultured human (MCF-7) breast cancer cells. J Steroid Biochem 1989;33:515–519. [PubMed: 2811361]
16. McLaughlin WH, Milius RA, Pillai KMR, Edasery JP, Blumenthal RD, Bloomer WD. Cytotoxicity of receptor-mediated 16a-[^{125}I]iodoestradiol in cultured MCF-7 human breast cancer cells. J Natl Cancer Inst 1989;81:437–440. [PubMed: 2918551]
17. Epperly MW, Damodaran KM, McLaughlin WH, Pillai KM, Bloomer WD. Radiotoxicity of 17-alpha-[^{125}I]iodovinyl-11-beta-methoxyestradiol in MCF-7 human breast cancer cells. J Steroid Biochem Mol Biol 1991;39:729–734. [PubMed: 1958509]
18. Beckmann MW, Scharl A, Rosinsky BJ, Holt JA. Breaks in DNA accompany estrogen-receptor-mediated cytotoxicity from 16-alpha[^{125}I]iodo-17 beta-estradiol. J Cancer Res Clin Oncol 1993;119:207–214. [PubMed: 8423195]
19. DeSombre ER, Mease RC, Hughes A, Harper PV, DeJesus OT, Friedman AM. Bromine-80m-labeled estrogens: Auger electron-emitting, estrogen receptor-directed ligands with potential for therapy of estrogen receptor-positive cancers. Cancer Res 1988;48:899–906. [PubMed: 3338083]
20. DeSombre ER, Shafii B, Hanson RN, Kuivanen PC, Hughes A. Estrogen receptor-directed radiotoxicity with Auger electrons: specificity and mean lethal dose. Cancer Res 1992;52:5752–5758. [PubMed: 1394199]
21. Schwartz JL, Mustafi R, Hughes A, DeSombre ER. DNA and chromosome breaks induced by iodine-123-labeled estrogen in Chinese hamster ovary cells. Radiat Res 1996;46:151–158. [PubMed: 8693065]
22. DeSombre ER, Hughes A, Landel CC, Greene G, Hanson R, Schwartz JL. Cellular and subcellular studies of the radiation effects of Auger electron-emitting estrogens. Acta Oncologica 1996;35:833–840. [PubMed: 9004760]

23. Kassis AI, Adelstein SJ, Haydock C, Sastry KSR, McElvany KD, Welch MJ. Lethality of Auger electrons from the decay of bromine-77 in the DNA of mammalian cells. Radiat Res 1982;90:362–373. [PubMed: 7079468]
24. Tang L. Radionuclide Production and Yields at Washington University School of Medicine. Q J Nucl Med Mol Imag. [in press]
25. Cui X, Schiff R, Arpino G, Osborne CK, Lee AV. Biology of progesterone receptor loss in breast cancer and its implications for endocrine therapy. J Clin Oncol 2005;23:7721–7735. [PubMed: 16234531]
26. Osborne CK, Schiff R, Arpino G, Lee AS, Hilsenbeck VG. Endocrine responsiveness: understanding how progesterone receptor can be used to select endocrine therapy. Breast 2005;14:458–465. [PubMed: 16236516]
27. Horowitz KB. The Structure and Function of Progesterone Receptors in Breast Cancer. J Steroid Biochem 1987;27:447–457. [PubMed: 3320537]
28. Santen R, Manni A, Harvey H, Redmond C. Endocrine treatment of breast cancer in women. Endocrine Rev 1990;11:221–265. [PubMed: 2194783]
29. Gelbfish GA, Davison AL, Kopel S, Schreibmen B, Gelbfish JS, Degenshein GA, et al. Relationship of Estrogen and Progesterone Receptors to Prognosis in Breast Cancer. Ann Surg 1988;207:75–79. [PubMed: 3337566]
30. Furr BJA, Jordan VC. The Pharmacology and Clinical Uses of Tamoxifen. Pharmacol Ther 1984;25:127–205. [PubMed: 6438654]
31. Noguchi S, Miyauchi K, Nishizawa Y, Koyama H. Induction of Progesterone Receptor with Tamoxifen in Human Breast Cancer with Special Reference to its Behavior over Time. Cancer 1988;61:1345–1349. [PubMed: 2964264]
32. Howell A, Harland RNL, Barnes DM, Baildam AD, Wilkinson MJS, Hayward E, et al. Endocrine Therapy for Advanced Carcinoma of the Breast: Relationship Between the Effect of Tamoxifen upon Concentrations of Progesterone Receptor and Subsequent Response to Treatment. Cancer Res 1987;47:300–304. [PubMed: 3791215]
33. Namer M, Lalanne C, Baulieu E. Increase of Progesterone Receptor by Tamoxifen as a Hormonal Challenge Test in Breast Cancer. Cancer Res 1980;40:1750–1752. [PubMed: 7371003]
34. Zhou D, Carlson KE, Katzenellenbogen JA, Welch MJ. Bromine-and iodine-substituted 16α,17α-dioxolane progestins for breast tumor imaging and radiotherapy: synthesis and receptor binding affinity. J Med Chem 2006;49:4737–4744. [PubMed: 16854080]
35. Buckman BO, Bonasera TA, Kirschbaum KS, Welch MJ, Katzenellenbogen JA. Fluorine-18-labeled progestin 16α,17α-dioxolanes: development of high-affinity ligands for the progesterone receptor with high in vivo target site selectivity. J Med Chem 1995;38:328–337. [PubMed: 7830275]
36. Kochanny MJ, VanBrocklin HF, Kym PR, Carlson KE, O'Neil JP, Bonasera TA, et al. Fluorine-18 labeled progestin ketals: synthesis and target tissue uptake selectivity of potential imaging agents for receptor-positive breast tumors. J Med Chem 1993;36:1120–1127. [PubMed: 8487253]
37. Denat F, Gaspard-Iloughmane H, Dubac J. An easy one-pot synthesis of Group 14 C-metalated 2(or 3)-furan-and thiophenecarboxaldehydes. Synthesis 1992;10:954–956.
38. Vijaykumar D, Wang M, Kirschbaum KS, Katzenellenbogen JA. An Efficient Route for the Preparation of a 21-Fluoro Progestin-16α,17α-Dioxolane, a High-Affinity Ligand for PET Imaging of the Progesterone Receptor. J Org Chem 2002;67:4904–4910. [PubMed: 12098304]
39. Van Den Bossche B, Van de Wiele C. Receptor imaging in oncology by means of nuclear medicine: current status. J Clin Oncol 2004;22:3593–3607. [PubMed: 15337810]
40. Katzenellenbogen, JA.; Heiman, DF.; Carlson, KE.; Lloyd, JE. In vivo and in vitro Steroid Receptor Assays in the Design of Estrogen Radiophamaceuticals. In: Eckelman, WC., editor. Receptor-Binding Radiotracers. Vol. 1. Boca Raton, FL: CRC; 1982. p. 93-126.
41. Dehdashti F, McGuire AH, Van Brocklin HF, Siegel BA, Andriole DP, Griffeth LK, et al. Assessment of 21-[^{18}F]fluoro-16 alpha-ethyl-19-norprogesterone as a positronemitting radiopharmaceutical for the detection of progestin receptors in human breast carcinomas. J Nucl Med 1991;32:1532–1537. [PubMed: 1869974]

42. Verhagen A, Studeny M, Luurtsema G, Visser GM, De Goeij CC, Sluyser M, et al. Metabolism of a [^{18}F]fluorine labeled progestin (21-[^{18}F]fluoro-16 alpha-ethyl-19-norprogesterone) in humans: a clue for future investigations. Nucl Med Biol 1994;7:941–952. [PubMed: 9234348]
43. Pomper MG, VanBrocklin H, Thieme AM, Thomas RD, Kiesewetter DO, Carlson KE, et al. 11β-Methoxy-, 11β-Ethyl- and 17α-Ethynyl-Substituted 16α-Fluoroestradiols: Receptor-Based Imaging Agents with Enhanced Uptake Efficiency and Selectivity. J Med Chem 1990;33:3143–3155. [PubMed: 1701833]
44. VanBrocklin HF, Pomper MG, Carlson KE, Welcη MJ, Katzevellenbogen JA. Preparation and Evaluation of 17-Ethynyl-substituted 16α-[^{18}F]Fluoroestradiols: Selective Receptor-based PET Imaging Agents. Nucl Med Biol 1992;19:363–374.
45. VanBrocklin HF, Rocque PA, Lee HV, Carlson KE, Katzenellenbogen JA. 16β-[^{18}F] Fluoromoxestrol: A Potent, Metabolically Stable Positron Emission Tomography Imaging Agent for Estrogen Receptor Positive Human Breast Tumors. Life Sciences 1993;53:811–819. [PubMed: 8355567]
46. Hanson, RN. The Influence of Structure Modification on the Metabolic Transformations of Radiolabeled Estrogen Derivatives. In: Nunn, A., editor. Radiopharmaceutical: Chemistry and Pharmacology. New York: Marcel Dekker; 1992. p. 333-364.
47. Soremark R, Ullberg S. Distribution of bromide in mice. An autoradiographic study with Br-82. Int J Appl Radiat Isot 1960;8:192–197.
48. Lee H, Finck BN, Jones LA, Welch MJ, Mach RH. Synthesis and evaluation of a bromine-76-labeled PPARγ antagonist 2-bromo-5-nitro-N-phenylbenzamide. Nucl Med Biol 2006;33:847–854. [PubMed: 17045164]
49. Müller K, Faeh C, Diederich F. Fluorine in pharmaceuticals: looking beyond intuition. Science 2007;317:1881–1886. [PubMed: 17901324]
50. Mathias CJ, Welch MJ, Katzenellenbogen JA, Brodack JW, Kilbourn MR, Carlson KE, et al. Characterization of the uptake of 16α-([^{18}F]fluoro)-17β-estradiol in DMBA-induced mammary tumors. Int J Rad Appl Instrum B 1987;14:15–25. [PubMed: 3108199]

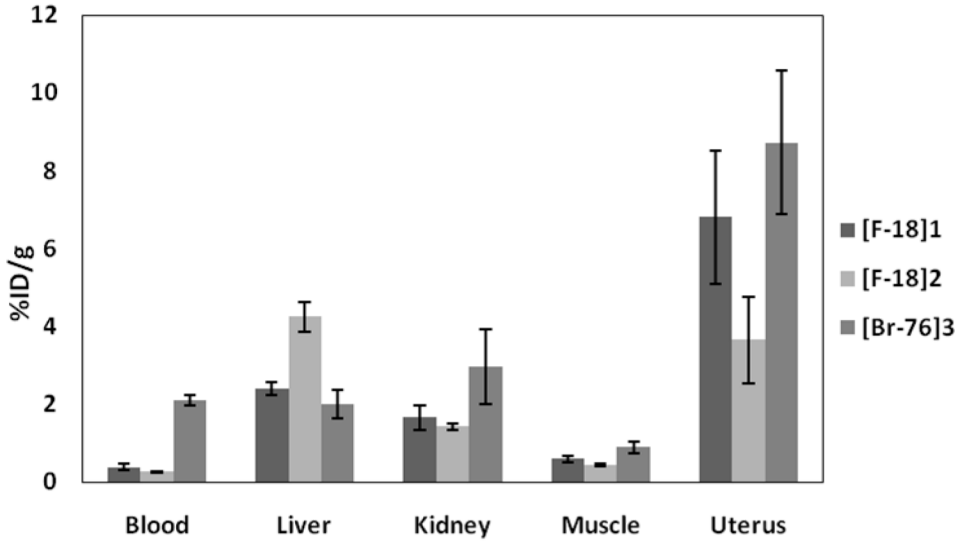

Figure 1.
Comparison of the tissue biodistribution of [^{18}F]**1**, [^{18}F]**2**, and [^{76}Br]**3** at 1 h post-injection

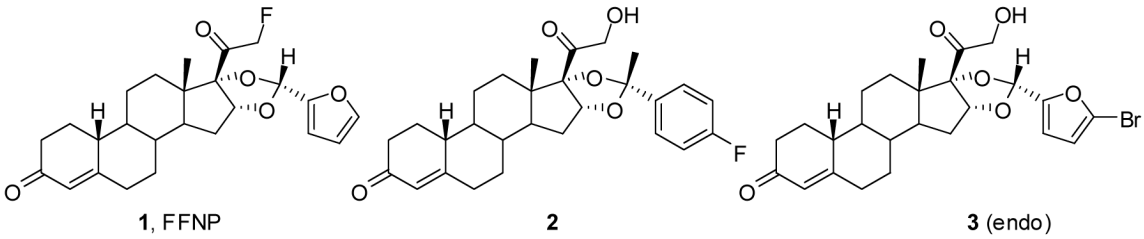

Scheme 1.
Progestin 16α,17α-dioxolanes

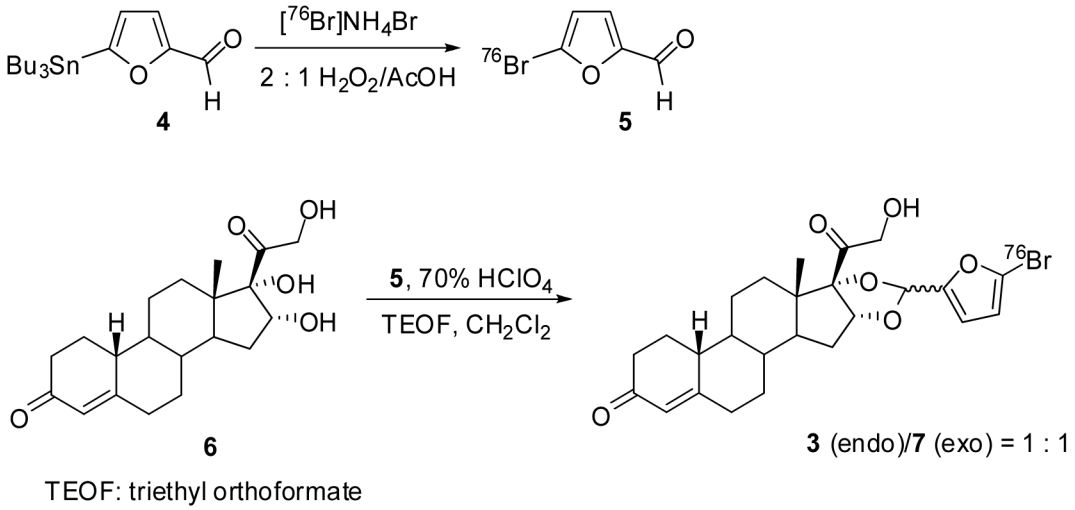

Scheme 2.
Scheme for the radiolabeling of [^{76}Br]**3**

Table 1

Fraction of ^{76}Br species in various tissues of estrogen-primed immature female rats

	Fraction of [^{76}Br] species (%)[a, b]															
	Uterus				Blood				Muscle				Liver			
Time	**1 m**	**1 h**	**3 h**	**24 h**	**1 m**	**1 h**	**3 h**	**24 h**	**1 min**	**1 h**	**3 h**	**24 h**	**1 m**	**1 h**	**3 h**	**24 h**
[^{76}Br]**3**	100	80	67.5	40	100	9	9	0	100	60	-	-	58.5	31.5	19.5	-
[^{76}Br]**8**	0	0	14.5	0	0	24.5	0	0	0	0	-	-	14.5	33.5	16	-
[^{76}Br]Br^{-}	0	20	17	60	0	66.5	91	100	0	40	-	-	27	35	63	-
Extraction (%)	94	93.5	90	88	85.5	79.5	80	79	90.5	82.5	86	89	83	73.5	74	76

[a] Determined by radio-TLC: silica plate/ethyl acetate, R_f = 0.6, 0.3, 0 for **3, 8** (the more polar metabolite), and bromide, respectively

[b] -: Under detection limit.

Table 2

Tissue biodistribution of [^{76}Br]**3** in estrogen-primed immature female rats

	Percent injected dose/g ± SD[a] n = 4			
	15 min (n = 3)	**1 h**	**3 h**	**24 h**
Blood	2.51 ± 0.58	2.11 ± 0.14	2.24 ± 0.38	1.52 ± 0.24
Liver	4.22 ± 0.87	2.01 ± 0.37	1.49 ± 0.26	0.60 ± 0.09
Spleen	1.34 ± 0.02	1.43 ± 0.82	1.07 ± 0.12	0.74 ± 0.15
Kidney	4.73 ± 0.84	2.96 ± 0.96	1.72 ± 0.21	1.01 ± 0.18
Muscle	1.38 ± 0.23	0.89 ± 0.16	0.71 ± 0.11	0.45 ± 0.11
Uterus	8.22 ± 0.63	8.72 ± 1.84	5.52 ± 1.84	1.18 ± 0.22
Uterus/blood	3.40 ± 0.83	4.11 ± 0.73	2.42 ± 0.36	0.77 ± 0.04
Uterus/muscle	6.08 ± 1.03	9.82 ± 1.57	7.67 ± 1.30	2.66 ± 0.32

[a] SD: standard deviation.

[b] 24 h and 3 h estradiol treatment before injection of [^{76}Br]**3**; 7 μCi/100 μL 15% ethanol/saline; Specific activity: > 400 mCi/μmol

Table 3

Tissue biodistribution of [^{76}Br]**3** in estrogen-primed immature female rats: blocking study

	Percent injected dose/g ± SD[a] n = 4			
	1 h	**1 h (block)**	**3 h**	**18 h**
Blood	2.10 ± 0.48	1.89 ± 0.18	1.76 ± 0.08	1.19 ± 0.19
Liver	2.39 ± 0.19	2.18 ± 0.21	1.18 ± 0.15	0.53 ± 0.07
Spleen	0.98 ± 0.08	0.95 ± 0.11	0.88 ± 0.05	0.59 ± 0.08
Kidney	2.32 ± 0.36	3.37 ± 0.48	1.31 ± 0.04	0.70 ± 0.12
Muscle	0.86 ± 0.10	0.81 ± 0.13	0.60 ± 0.09	0.41 ± 0.11
Uterus	5.26 ± 0.35	2.43 ± 0.34	2.69 ± 0.20	0.71 ± 0.14
Ovaries	3.54 ± 0.56	2.06 ± 0.44	1.91 ± 0.38	0.64 ± 0.12
Uterus/blood	2.65 ± 0.88	1.28 ± 0.12	1.54 ± 0.17	0.60 ± 0.04
Uterus/muscle	6.21 ± 1.12	3.01 ± 0.24	4.58 ± 0.65	1.74 ± 0.14

[a] SD: standard deviation.

[b] 3 h estradiol treatment before injection of [^{76}Br]**3**; 2~3 μCi/100μL 15% ethanol/saline specific activity: 1250 mCi/μmol

Table 4

Tissue biodistribution of [^{76}Br]**3** in estrogen-primed immature female rats: dose study

	Percent injected dose/g ± SD[a] *n* = 4		
	1 h (0.8 μCi)	**1 h (2 μCi)**	**1 h (40 μCi))**
Blood	2.16 ± 0.55	1.83 ± 0.16	1.86 ± 0.40
Liver	2.26 ± 0.28	2.07 ± 0.36	1.99 ± 0.45
Spleen	1.10 ± 0.15	0.93 ± 0.05	1.07 ± 0.32
Kidney	2.60 ± 0.99	1.84 ± 0.21	2.38 ± 0.98
Muscle	0.70 ± 0.06	0.78 ± 0.16	0.87 ± 0.42
Uterus	6.00 ± 1.44	5.42 ± 1.14	5.26 ± 1.04
Ovaries	3.35 ± 0.42	2.83 ± 0.28	3.36 ± 0.66
Uterus/blood	2.79 ± 0.21	2.97 ± 0.64	2.96 ± 1.06
Uterus/muscle	8.65 ± 2.15	7.23 ± 2.19	7.16 ± 3.67

[a] SD: standard deviation.

[b] 48h and 24 h estradiol treatments before injection of [^{76}Br]**3**; 100μL 15% ethanol/saline; specific activity: 200 mCi/μmol

Table 5

Comparison of the tissue biodistribution of ^{18}F and ^{76}Br labeled progestins in estrogen-primed immature female rats

	Percent injected %ID/g ± SD[a]					
	1 (1 h)	**2 (1 h)**	**3 (1 h)**	**1 (3 h)**	**2 (3 h)**	**3 (3 h)**
Blood	0.38 ± 0.08	0.26 ± 0.02	2.11 ± 0.14	0.19 ± 0.07	0.10 ± 0.02	2.24 ± 0.38
Liver	2.40 ± 0.18	4.25 ± 0.39	2.01 ± 0.37	1.65 ± 0.25	1.36 ± 0.22	1.49 ± 0.26
Kidney	1.66 ± 0.32	1.42 ± 0.08	2.96 ± 0.96	0.73 ± 0.26	0.45 ± 0.10	1.72 ± 0.21
Muscle	0.59 ± 0.08	0.44 ± 0.04	0.89 ± 0.16	0.26 ± 0.08	0.16 ± 0.09	0.71 ± 0.11
Uterus	6.80 ± 1.70	3.65 ± 1.11	8.72 ± 1.84	7.83 ±1.41	3.86 ± 0.99	5.52 ± 1.84
Uterus/blood	18.2 ± 4.9	14.0 ± 4.2	4.11 ± 0.73	48.0 ± 24.4	38.0 ± 8.3	2.42 ± 0.36
Uterus/muscle	11.6 ± 3.3	8.20 ± 2.5	9.82 ± 1.57	32.2 ± 10.9	27.9 ± 9.5	7.67 ± 1.30
RBA (%)[b]	190	240	65			
Log *P*o/w[c]	3.87	4.92	5.09 ± 0.84[d]			
SA[e]	> 1200[*]	409	> 400			

[a] SD: standard deviation; Data for **1** and **2** are from ref. 35.

[b] RBA: relative binding affinity, relative to R5020 (100%)

[c] Log $P_{O/W}$: log of octanol/water partition coefficient (ref. 35)

[d] Calculated using ACD LogP software (ref. 34)

[e] SA: specific activity, determined by HPLC

[*] effective SA (ref. 35).